

MEASUREMENTS OF COSMIC-RAY AIR SHOWER DEVELOPMENT  
AT ENERGIES ABOVE  $10^{17}$  eVG. L. CASSIDAY, R. COOPER, S. C. CORBATÓ, B. R. DAWSON, J. W. ELBERT, B. E. FICK, K. D. GREEN,  
D. B. KIEDA, S. KO, D. F. LIEBING, E. C. LOH, M. H. SALAMON, J. D. SMITH, P. SOKOLSKY,  
P. SOMMERS, S. B. THOMAS, S. X. WANG, AND B. WHEELER

Physics Department, University of Utah

Received 1989 August 2; accepted 1989 December 20

## ABSTRACT

We present measurements of the depth of maximum for extensive air showers (EAS) produced by cosmic-ray nuclei with energies above  $10^{17}$  eV. The air showers were observed using the University of Utah's Fly's Eye detectors operating in stereo mode. Measurements of the atmospheric nitrogen fluorescence light generated by EAS have been used to obtain longitudinal development curves of individual showers and, in particular, the depth of maximum of each shower. The data imply an elongation rate of  $69.4 \pm 5.0$  g cm $^{-2}$  per decade above  $10^{17}$  eV without correction for triggering and resolution effects. These effects contribute approximately  $+5$  g cm $^{-2}$  per decade to the apparent elongation rate. The distribution of depths of shower maximum has a mean value of  $690 \pm 3$  g cm $^{-2}$  (with an estimated systematic uncertainty of  $\pm 20$  g cm $^{-2}$ ) and a width (standard deviation) of  $85 \pm 2$  g cm $^{-2}$  for showers with energies above  $3 \times 10^{17}$  eV. The tail of the distribution has a logarithmic decrement of  $\lambda = 70 \pm 14$  g cm $^{-2}$ . Comparison with predictions for a pure proton and a pure iron flux indicates that the data are not consistent with either and are instead consistent with a mixture. This will be further discussed in an upcoming publication by Gaisser *et al.*

*Subject heading:* cosmic rays: general

## I. INTRODUCTION

A knowledge of the elemental composition of ultra-high-energy cosmic rays is necessary in order to understand the origin of these particles. However, the measurement of the composition at these energies is notoriously difficult. Because of the very low flux, measurements are by necessity indirect and make use of the extensive air showers (EAS) produced by the primary cosmic rays in the atmosphere. Typically, experiments attempt to determine the nature of the primary particle by measuring the position in the atmosphere of the air shower maximum. The depth of shower maximum,  $X_{\max}$  (in g cm $^{-2}$ ), depends on the primary energy and the mass of the incoming primary cosmic ray, and the nature of the interactions of elementary particles at extremely high energies. For a fixed energy, heavy nuclei produce showers which develop more rapidly (smaller depth of maximum) than proton produced showers. In simple terms, the reason for this can be attributed to two effects. First, the interaction length of the cosmic ray entering the atmosphere is smaller for the more massive primaries, and second, the primary energy of the particle is shared between its constituent nucleons during the first few interactions. Each nucleon produces a subshower whose penetrating power depends on the fraction of the primary energy originally given to the nucleon. The superposition of all such subshowers will be a less penetrating shower than one produced by a single nucleon with the entire primary energy. The effects of the shorter interaction length and the superposition of a number of subshowers also mean that heavy nuclei produce showers that have smaller fluctuations in development from shower to shower of the same energy.

## II. EXPERIMENTAL DETAILS

The Fly's Eye detectors are located at an atmospheric depth of 860 g cm $^{-2}$  in the western desert of Utah at Dugway

Proving Grounds,  $\sim 160$  km southwest of Salt Lake City. The details of the experiment are given elsewhere (Baltrusaitis *et al.* 1985), but we will give a brief overview here. There are two Fly's Eye detectors, Fly's Eye I and Fly's Eye II, separated by a distance of 3.4 km. The data discussed in this report represent events detected by both detectors simultaneously. This "stereoscopic" view of air showers significantly improves the geometrical reconstruction of the data, important in studies sensitive to position dependencies such as composition.

Fly's Eye I consists of 67 1.6 m diameter mirrors, each with 12 or 14 phototubes at its focus. Each of the 880 phototubes in the Eye views a different 5°5 diameter hexagonal area of the night sky. Fly's Eye II consists of 36 mirrors and 464 tubes, and it views half of the night sky in the direction of Fly's Eye I. The second detector has been operating in its present configuration since 1986 November. The detectors are unique since they constitute the only cosmic-ray instrument capable of directly measuring individual air shower longitudinal development profiles. The technique is also desirable because a large collecting area is available. The detector is operated during clear moonless nights, giving a duty cycle of  $\sim 10\%$ .

Showers are detected via the nitrogen fluorescence they induce in the atmosphere. While the efficiency of the fluorescence process is low, the number of particles in large air showers makes the technique feasible for primary energies above  $\sim 10^{17}$  eV. Unlike the more intense Cerenkov light, the fluorescence (or scintillation) light is emitted isotropically around the shower axis, allowing detection at large distances from the shower. The growth and decay of an air shower can be traced as it passes down through the atmosphere. The actual shower development profile is obtained from the measured light intensities by properly accounting for the distance between the EAS light source and the detector, making corrections for atmospheric attenuation and scattering and using the known efficiency of the fluorescence process. Determination of

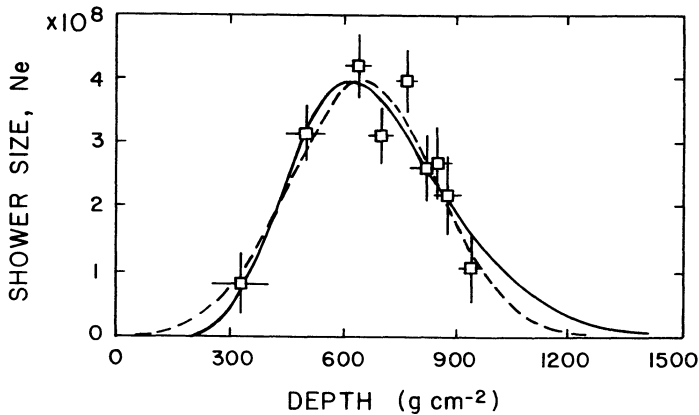


FIG. 1.—A typical shower development profile as measured by the stereo Fly's Eyes. Two fits to the data are shown, Gaussian (*dashed line*) and Gaisser-Hillas (*solid line*). Results from the Gaussian fit given an energy of  $(4.6 \pm 0.4) \times 10^{17}$  eV and a depth of maximum of  $650 \pm 39$  g cm $^{-2}$ .

this profile provides an almost model-independent measurement of the energy of the primary cosmic ray as well as a direct measurement of the depth of shower maximum. A typical measured shower profile is shown in Figure 1.

Both the average value and the width of the distribution of depths of maximum can be used in a composition study. The tail of the distribution can also be used to determine the fluctuations in the depth of first interaction and hence the proton-air inelastic cross section, provided that the flux has a significant protonic component.

### III. INVESTIGATION OF DETECTOR RESOLUTION AND MEASUREMENT SYSTEMATICS

We have developed a detailed Monte Carlo simulation program to model the performance of the two Fly's Eyes. The program takes previously generated one-dimensional shower development profiles (Gaisser and Stanev 1989) and uses the known efficiencies for nitrogen fluorescence and Cerenkov light production (Baltrusaitis *et al.* 1985) to calculate the light produced by each shower. Solid angle effects and Rayleigh and aerosol scattering processes are taken into account in order to calculate the amount of light arriving at the detectors. The optical and electronic characteristics of the detectors are modeled to produce an output consisting of a list of firing photomultipliers with the associated pulse amplitude and timing information. These results are then passed through the standard analysis procedure, giving a simulated data sample that reflects the triggering acceptance and reconstruction resolution of the experiment.

The Monte Carlo analysis has successfully reproduced experimentally measured distributions including impact parameter and zenith angle distributions (Baltrusaitis *et al.* 1985), as well as the distributions of estimated errors in various parameters. As an example we show in Figure 2 the experimentally determined distribution of estimated error in  $X_{\max}$ . This error includes geometrical reconstruction errors as well as errors associated with the fitting of the longitudinal shower profile. Included in Figure 2 is the same distribution from a simulation of the detectors, indicating a very good agreement between the experimental data and the Monte Carlo results.

In our study of the composition question (Gaisser *et al.* 1990) we use the Monte Carlo procedure to calculate the expected  $X_{\max}$  distribution for particular mixtures of primary

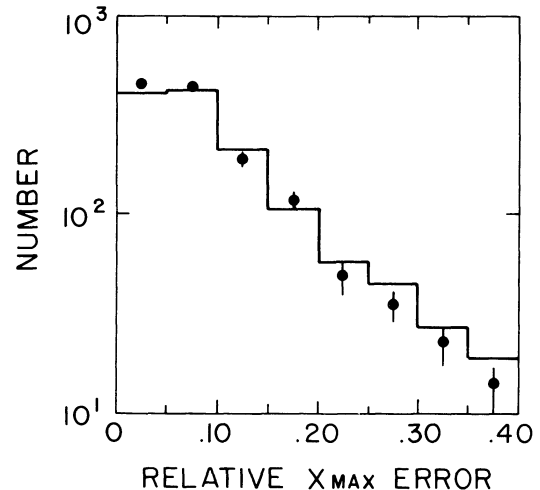


FIG. 2.—The distributions of estimated relative error in depth of maximum for data (mean of 0.12, standard deviation of 0.13) (*histogram*) and simulated events (mean of 0.11, standard deviation of 0.13) (*filled circles*). For  $E > 3 \times 10^{17}$  eV with all viewing angles  $> 20^\circ$ .

components under various assumptions about the particle interaction model. However, here we present some fundamental results regarding detector resolution and triggering acceptance. Figure 3 shows the depth of maximum resolution function determined for a sample of Monte Carlo generated showers with energies above  $3 \times 10^{17}$  eV viewed in stereo. No quality cuts have been applied to the reconstructed data. We have found that this function is independent of the absolute value of  $X_{\max}$  over the range of values detected. The width of the resolution function can be expressed in terms of a standard deviation of  $65$  g cm $^{-2}$ .

The Fly's Eye detection efficiency varies as a function of the depth of maximum. Showers with small depths of maximum develop at large distances from the detector and are therefore less efficiently seen. On the other hand, showers with very large depths of maximum may hit ground level before shower maximum is reached, especially if they develop vertically. Both of these effects are seen in Figure 4. Here we show the Fly's Eye

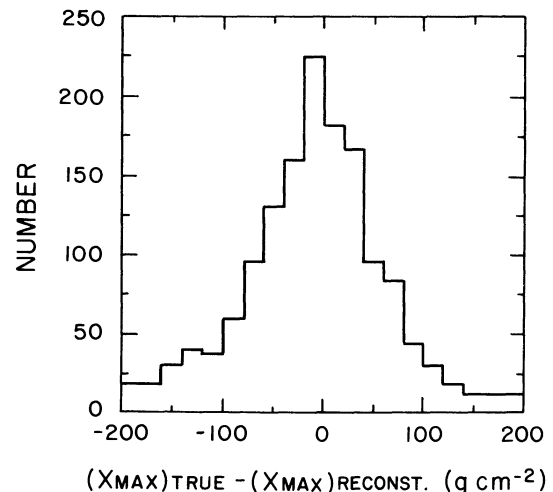


FIG. 3.—The depth of maximum resolution function determined using the detector Monte Carlo (no cuts). The distribution has a standard deviation of  $65$  g cm $^{-2}$ .

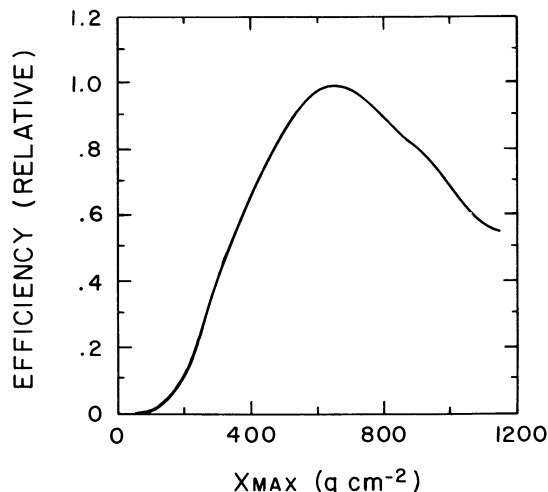


FIG. 4.—The relative depth of maximum triggering efficiency for showers with energies above  $3 \times 10^{17}$  eV.

triggering efficiency as a function of  $X_{\max}$ , normalized to 1.0 at the peak efficiency. This Monte Carlo result represents showers seen in stereo mode with energies above  $3 \times 10^{17}$  eV. (For a shower to “trigger” the detector, shower maximum must be seen). Note that the efficiency is not changing rapidly in the region between 500 and 800  $\text{g cm}^{-2}$ , the region of the atmosphere expected to be of most interest for cosmic rays of this energy.

A thorough investigation has been made of the possible systematic errors associated with the determination of the depth of maximum. The main areas are listed below.

We have made a study of the reliability of the first step in the analysis procedure, the geometric reconstruction of our stereo events (the determination of impact parameter, zenith angle, etc.). A series of vertical xenon flashers arranged around the two eyes provide a constant monitor of our performance in this area. These flashers generate regular shower-like tracks of light with impact parameters of 1–5 km. We also periodically use moderate power nitrogen lasers ( $\lambda = 337$  nm) to investigate reconstruction at larger impact parameters and various zenith angles. The results of these studies (Baltrusaitis *et al.* 1987a) have proven the accuracy of the stereo technique and have provided checks of the estimated error distributions. We find that there are no significant systematic errors in stereo geometrical reconstruction and that the estimated reconstruction errors are consistent with actual errors.

Laser shots also provide information on the scattering of light in the atmosphere. While we have every confidence in our treatment of classical Rayleigh scattering, these shots have provided a check of the corrections we make for aerosol (Mie) scattering in the lower atmosphere. The reconstruction of a variety of fixed-energy laser shots fired with various orientations has confirmed our assumptions about the angular distribution of this type of scattering as well as providing a measurement of the aerosol density in the Dugway area. We note that since most showers detected in stereo have impact parameters between 1 and 4 km, and the typical Mie scattering length is 14 km (Elterman and Toolin 1965), the sensitivity of the depth of maximum distribution to the concentration of aerosols is small. Reanalysis of the data using an aerosol concentration of 10 times the nominal value results in a new average depth of maximum that is shifted by only 10  $\text{g cm}^{-2}$ .

Independent measurements using light beams of known intensity are used to determine the nightly aerosol variations. A factor of 10 increase in aerosol concentration is far greater than the day-to-day variation experienced at Dugway.

In studies of air shower development it is necessary to have an adequate model of the density profile of the atmosphere. We use a fit (Gaisser *et al.* 1981) to the US Standard Atmosphere and have checked this against daily radiosonde measurements of the profile made at Salt Lake City Airport, 160 km from Dugway. We find that the standard atmosphere is an excellent match to the average yearly profile at our location and that the seasonal variations in column density, which amount to  $\pm 5$ –10  $\text{g cm}^{-2}$  at any given height level, are small compared with the  $X_{\max}$  resolution of the detector.

The light from air showers observed by the Fly’s Eyes is generally produced by nitrogen fluorescence and is emitted isotropically. If, however, part of the shower is viewed at a small angle to the shower axis, a significant (and usually overwhelming) fraction of the light will be due to the Cerenkov process. Cerenkov light is a contaminant in this particular experiment, and its effect must be removed in the analysis procedure in order to retrieve the image of the shower profile. (Fortunately, only a certain class of events have geometries which result in this problem, and the Cerenkov light that is seen is attenuated somewhat by the band pass optical filters placed in front of the phototubes). In order to correct for this contamination, both the intensity and the angular distribution of the light must be known. The angular distribution is determined primarily by the angular distribution of the shower electrons that produce the light. We have measured the angular distribution of Cerenkov light from large air showers (Baltrusaitis *et al.* 1987b) and found that it implies a value of the electron multiple scattering parameter of  $\theta_0 = 4^\circ 0 \pm 1^\circ 2$ , in agreement with Monte Carlo calculations. The intensity of the light is proportional to the total track length of the super-threshold shower particles. We have varied these parameters over reasonable ranges to check the sensitivity of the  $X_{\max}$  distribution to the choices of this sort. The effect was found to be small. The average  $X_{\max}$  of the data set change by  $\pm 15$   $\text{g cm}^{-2}$  for a change in the Cerenkov angular distribution parameter,  $\theta_0$ , by one standard deviation in each direction. A similar change was found when the intensity of the Cerenkov light was assumed to be larger or smaller by a factor of 2.

One can avoid the problem of direct Cerenkov light contamination by only looking at events which are viewed at large angles to the shower axis. We define the “viewing angle” of any phototube as the angle between the pointing direction of the tube and the shower axis, and we have investigated the effect of requiring that all viewing angles in an event be greater than  $20^\circ$ . This cut removes any concern about the effect of direct Cerenkov contamination and also effectively applies a zenith angle cut to the data, removing large zenith angle events which suffer from large uncertainties in the depth of maximum. (For these events, small errors in reconstructed zenith angle translate into large errors in depth of maximum). The application of this cut does not significantly change the average depth of maximum of the data set (the shift is less than 10  $\text{g cm}^{-2}$ ), but it does remove some spurious events from the large  $X_{\max}$  end of the distribution.

In addition to providing a superior method of geometrical reconstruction, the stereo technique offers two independent measurements of the shower profile. The normal procedure is to average the two profiles for our measurements of  $X_{\max}$ , but



we have studied the individual profiles to look for systematic differences. (In this study we retained the geometrical parameters determined from the stereo reconstruction). Taken separately, the two profiles systematically give depths of maximum which are different by  $\sim 15 \text{ g cm}^{-2}$ . This is not surprising given that the two Eyes are physically different—Fly's Eye II views only half of the night sky. One can take this result as an upper limit on the systematic error in  $X_{\text{max}}$  introduced by averaging the response of two detectors.

We have compared two functional forms for the fitting of the shower development profiles. The first, the so called Gaisser-Hillas parameterization (Gaisser and Hillas 1977), is believed to be a realistic representation of an average shower. However, we find that because of the detector's finite resolution, a simple Gaussian function fits the data just as well. The  $\chi^2$  distributions for the two fitting functions are very similar, but the fitting success rate is slightly higher for the Gaussian form. We have therefore used the latter function in the analysis of the data reported here. Studies of Monte Carlo-generated events show that on an event by event basis the Gaussian fit gives depths of maximum that are on average  $10 \text{ g cm}^{-2}$  deeper than the input value, while the Gaisser-Hillas fit gives depths that are on average  $10 \text{ g cm}^{-2}$  shallower. The real data also show this effect. The Gaussian form gives depths of maximum that are on average  $20 \text{ g cm}^{-2}$  deeper than the Gaisser-Hillas values. Thus when comparing the data with Monte Carlo-generated events, the systematic error involved with the choice of fitting function is seen to be negligible.

In summary, we have found that the largest possible source of systematic errors is in the treatment of Cerenkov light contamination. We have been able to eliminate the problem by making geometric cuts on the data sample. We estimate that the remaining sources of systematic error amount to shifts of no more than  $\pm 20 \text{ g cm}^{-2}$  in the average value of the depth of maximum.

#### IV. EXPERIMENTAL RESULTS

The stereo data discussed here were collected during the period between 1986 November (the beginning of operation of the completed Fly's Eye II) and 1988 August, the actual running time being  $\sim 1400$  hr. There have been two selection cuts applied to the data. The first, a requirement that the estimated relative error in the depth of maximum be less than 0.12 (the mean value of the error distribution; see Fig. 2), takes into account statistical errors in both the geometrical reconstruction and the fitting of the Gaussian shower profile. Making such a cut ensures that we are well away from any non-Gaussian tails in the error distribution which are difficult to model. The second is the Cerenkov light cut discussed above. An event is rejected if the viewing angle of any phototube in the event is less than  $20^\circ$ .

The elongation rate is a parameter measured in many studies of air shower development. It can be defined as the change in the average depth of maximum per decade of shower energy and is useful in detecting rapid changes in shower behavior over a particular energy range (Linsley and Watson 1981). Shower calculations (e.g., Elbert 1981) show that the elongation rate expected for a scaling model of interactions, constant hadronic cross sections and constant primary composition is  $\sim 100 \text{ g cm}^{-2}$  per decade. Different assumptions about the interaction model and changes in the composition with energy can both change the expected elongation rate. For example, departures from scaling and the introduction of cross

TABLE 1  
DEPTH OF MAXIMUM AS A FUNCTION OF ENERGY

| Energy Range (EeV) | Energy (EeV) | $X_{\text{max}}$ ( $\text{g cm}^{-2}$ ) | Width ( $\text{g cm}^{-2}$ ) | Number of Events |
|--------------------|--------------|---|------------------------------|------------------|
| 0.10–0.17          | 0.14         | $648 \pm 6.8 \pm 20$                    | $84 \pm 4.8$                 | 153              |
| 0.17–0.30          | 0.23         | $647 \pm 4.9 \pm 20$                    | $76 \pm 3.5$                 | 243              |
| 0.30–0.55          | 0.42         | $665 \pm 4.4 \pm 20$                    | $75 \pm 3.1$                 | 289              |
| 0.55–1.00          | 0.75         | $672 \pm 5.3 \pm 20$                    | $86 \pm 3.7$                 | 266              |
| 1.00–1.70          | 1.30         | $704 \pm 5.6 \pm 20$                    | $76 \pm 4.0$                 | 185              |
| 1.70–3.00          | 2.20         | $729 \pm 8.1 \pm 20$                    | $81 \pm 5.7$                 | 100              |
| >3.0               | 6.39         | $754 \pm 8.9 \pm 20$                    | $82 \pm 6.3$                 | 86               |

sections rising with energy both act to reduce the rate. Changes in composition as a function of energy could result in a rate larger or much smaller than the  $100 \text{ g cm}^{-2}$  figure, depending on whether the change decreases or increases the mean atomic mass of the primary particles.

The present data set has been broken up into seven energy regions as listed in Table 1. Here we show the average energy in each bin and the corresponding mean value of the depth of maximum. There are two errors given for each average depth of maximum—the statistical error and the estimate of possible systematic error. These data are plotted in Figure 5 along with the results from two Cerenkov light experiments. A least-squares fit to our seven data points (weighted by statistical errors) gives an elongation rate of  $69.4 \pm 5.0 \text{ g cm}^{-2}$  per decade from  $10^{17}$  eV to  $6 \times 10^{18}$  eV ( $\chi^2$  per d.f. = 2.72). We note that a simulated data sample with an input elongation rate of  $65 \text{ g cm}^{-2}$  (produced using an interaction model described at the end of this report) gives an elongation rate of  $70.3 \pm 3.1 \text{ g cm}^{-2}$  per decade after being passed through the detector Monte Carlo and reconstruction programs. Thus over the energy range of our measurement, the combination of triggering efficiency and resolution effects contribute to a systematic increase of the apparent elongation rate of only  $5 \text{ g cm}^{-2}$  per decade.

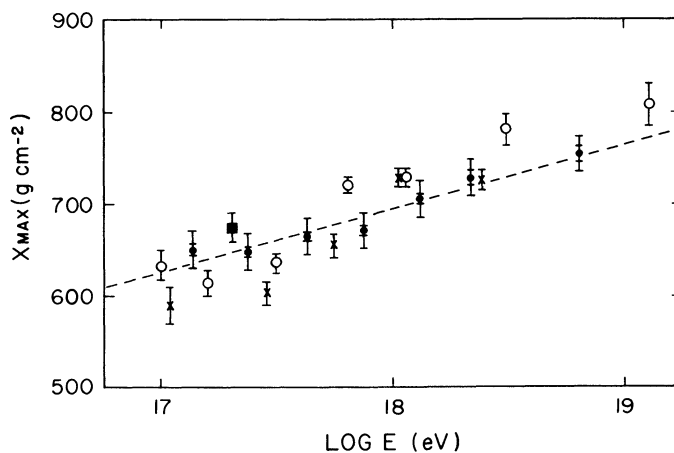


FIG. 5.—Depth of maximum vs. energy. Experimental points: this work (filled circles); Chantler *et al.* 1982 (filled square); Efimov *et al.* 1987 (open circles and crosses). The two sets of Soviet data represent two zenith angle ranges (open circles:  $\theta = 17^\circ$ ; crosses:  $\theta = 37^\circ$ ) and indicate the size of systematic errors in that experiment. The error bars on the Fly's Eye points represent both the statistical and systematic uncertainties listed in Table 1. The weighted least-squares fit to the Fly's Eye points is shown by the dashed line. The implied elongation rate is  $69.4 \pm 5.0 \text{ g cm}^{-2}$  per decade.

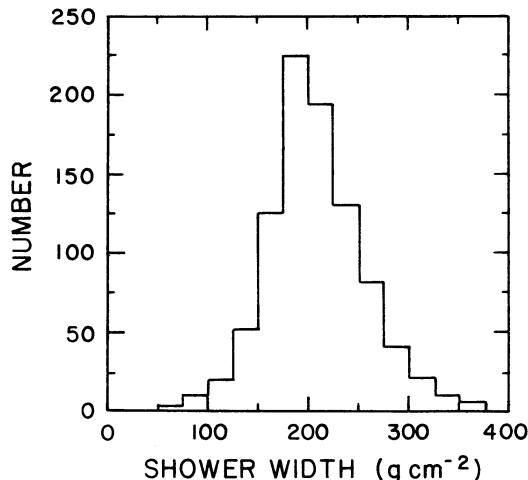


FIG. 6.—The distribution of shower widths for showers with energies larger than  $3 \times 10^{17}$  eV, estimated relative  $X_{\max}$  error less than 0.12 and all viewing angles larger than  $20^\circ$ . The parameter plotted is the standard deviation of the Gaussian shower profile function. The mean value of the distribution is  $207 \pm 2$  g cm $^{-2}$  with a width (standard deviation) of  $50 \pm 1$  g cm $^{-2}$ .

Also listed in the table are values for the widths (standard deviations) of the seven depth of maximum distributions. No attempt has been made to remove the effects of the finite detector resolution (see below).

We turn from the width of the depth of maximum distribution to the distribution of individual shower widths. The width is expressed in terms of the standard deviation of the Gaussian fitting function. The distribution of profile widths for showers with energies above  $3 \times 10^{17}$  eV is shown in Figure 6. Such an energy cut leaves a total of 926 events. The mean width of the showers is  $207 \pm 2$  g cm $^{-2}$  with a distribution standard deviation of  $50 \pm 1$  g cm $^{-2}$ . Unlike the depth of maximum, the shower width (defined as a Gaussian sigma or a full width at half-maximum) has only a small dependence on the primary composition since it is dominated by the electromagnetic component of the shower. The rate of growth of the width with

energy is expected to be small (a change of the order of 10 g cm $^{-2}$  from  $10^{17}$  eV to  $10^{18}$  eV; Linsley 1985). Because of the finite resolution of this experiment, our data show none of the expected correlation between  $X_{\max}$  and shower width.

Finally we come to the depth of maximum distribution. We are particularly interested in three features of the distribution; its mean value, its width, and the exponential slope of the large  $X_{\max}$  tail. The first two parameters have bearing on the composition issue, while the third offers information on the development fluctuations in the deeply penetrating showers, and hence on the proton-air inelastic cross section.

The depth of maximum distribution for the 926 events with energies above  $3 \times 10^{17}$  eV is shown in Figure 7a. The mean value of the depth of maximum is  $690 \pm 3$  g cm $^{-2}$  and the width (standard deviation) of the distribution is  $85 \pm 2$  g cm $^{-2}$ . Shown in Figure 7b is another depth of maximum distribution. It contains all the data of Figure 7a, with additional events from the period from 1988 August to December. We have not included these later data in any of our earlier discussions, since the detector electronics characteristics were changed in 1988 August, increasing the sensitivity of the detector to higher energy events. However, this change in the energy acceptance is not significant for measurements of the slope of the tail of the  $X_{\max}$  distribution, since the growth of the proton-air cross section with energy is known to be very slow. We find that the tail of the distribution can indeed be represented by an exponential of the form

$$N = N_0 \exp(-X_{\max}/\lambda)$$

with  $\lambda = 70 \pm 14$  g cm $^{-2}$  for  $X_{\max} \geq 850$  g cm $^{-2}$ . (The corresponding value for the data in Figure 7a is  $72 \pm 15$  g cm $^{-2}$ ). This stereo result is in agreement with our previously published result from single-Eye observations (Baltrusaitis *et al.* 1984).

Note that no attempt has been made to remove the finite detector resolution or acceptance effects from either distribution in Figure 7. Our preference has been to use our Monte

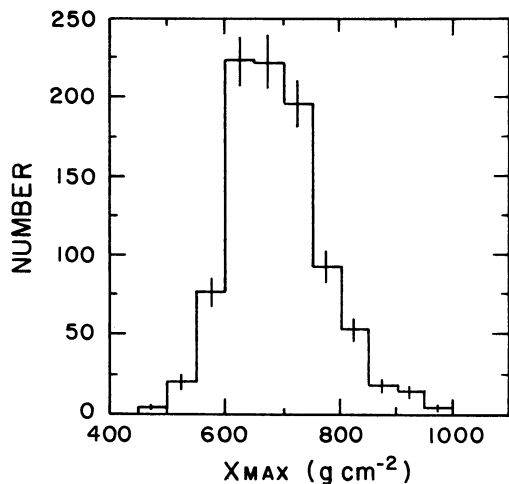


FIG. 7a

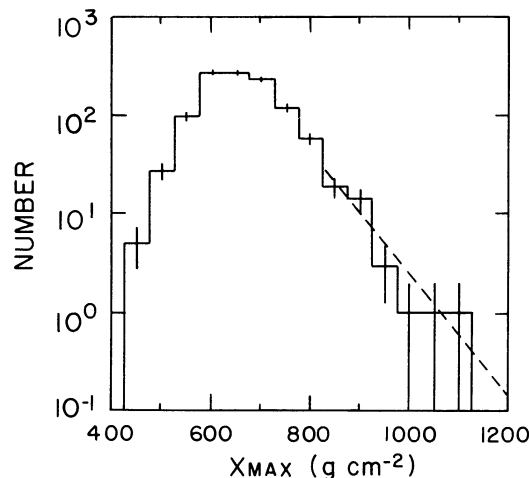


FIG. 7b

FIG. 7.—Depth of maximum distributions: (a) data from 1986 November until 1988 August; (b) same as (a), but with additional data up until 1988 December. The selection cuts for both plots are the same as those used in Fig. 6. In (a) the mean depth of maximum is  $690 \pm 3$  g cm $^{-2}$  with a distribution width (standard deviation) of  $85 \pm 2$  g cm $^{-2}$ . The dashed line in (b) represents the exponential fit to the tail of the distribution ( $X_{\max} \geq 850$  g cm $^{-2}$ ). See text.

Carlo program to produce simulated distributions that include the effects of resolution and detection efficiencies. It is then possible to extract estimates of the intrinsic composition mix and the proton-air inelastic cross section.

We present the results of one model here. Briefly, the model (Gaisser and Stanev 1989) assumes a mild scaling violation in the fragmentation region and cross sections that rise with  $\ln^2 s$ , where  $s$  is the square of the center of mass energy. This model is consistent with what is known about hadronic interactions at accelerator energies. Shower profiles representing iron and proton showers with energies above  $3 \times 10^{17}$  eV have been processed through the detector Monte Carlo and analysis routines and give the results shown in Table 2. Here we give the mean and width (standard deviation) of each distribution, which include the effects of triggering efficiencies and resolution. It is clear that the data cannot be represented by a pure composition of either protons or iron. The average depth of maximum of proton showers would have to be shifted by more than  $100 \text{ g cm}^{-2}$  in order to match the data. This shift is much larger than expected even in quite extreme models of hadronic interactions (Gaisser *et al.* 1990). A pure iron beam is inconsistent with the width of the experimental distribution. An interaction model allowing a broadening of the iron  $X_{\text{max}}$  distribution would naturally lead to a deeper average depth of maximum, one inconsistent with the data. A mixture of components is required to match both the mean *and* the width of the experimental  $X_{\text{max}}$  distribution.

TABLE 2  
DEPTH OF MAXIMUM RESULTS FROM ONE INTERACTION MODEL

| Distribution  | Average $X_{\text{max}}$<br>( $\text{g cm}^{-2}$ ) | Width<br>( $\text{g cm}^{-2}$ ) |
|---------------|--|---------------------------------|
| Protons ..... | $803 \pm 2$  | $80 \pm 1$                      |
| Iron .....    | $705 \pm 3$  | $66 \pm 2$                      |
| Data .....    | $690 \pm 3 \pm 20$                                 | $85 \pm 2$                      |

#### V. CONCLUSION

In this paper we have reported measurements of the depth of maximum of ultrahigh energy extensive air showers. The technique employed provides an opportunity to measure the development profiles of individual showers, allowing a straightforward and calculation-independent extraction of the depth of maximum. We have performed a study of the possible systematic errors present in the experiment and have found their magnitude to be small. The data are not compatible with either a pure proton or a pure iron composition. A detailed interpretation of the measured depth of maximum distribution, including a study of the model dependence of the conclusions, is in preparation (Gaisser *et al.* 1990).

Helpful discussions with T. K. Gaisser and T. Stanev are gratefully acknowledged. The National Science Foundation is thanked for its support of this research.

#### REFERENCES

- Baltrusaitis, R. M., *et al.* 1984, *Phys. Rev. Letters*, **52**, 1380.  
 ———. 1985, *Nucl. Instr. Meth.*, **A240**, 410.  
 ———. 1987a, *Proc. 20th Internat. Conf. Cosmic Rays* (Moscow), **2**, 428.  
 ———. 1987b, *J. Phys. G: Nucl. Phys.*, **13**, 115.  
 Chantler, M. P., Craig, M. A. B., McComb, T. J. L., Orford, K. J., Turver, K. E., and Walley, G. M. 1982, *J. Phys. G: Nucl. Phys.*, **8**, L51.  
 Efimov, N. N., *et al.* 1987, *Proc. 20th Internat. Conf. Cosmic Rays* (Moscow), **5**, 490.  
 Elbert, J. W. 1981, in *Proc. Paris Workshop on Cascade Simulations*, ed. J. Linsley and A. M. Hillas (College Station, TX: Texas Center for Advancement of Science and Technology), p. 7.  
 Elterman, L., and Toolin, R. B. 1965, *Handbook of Geophysics and Space Environments*, Air Force Cambridge Research Labs., Office of Aerospace Research (Cambridge, MA: USAF), Chap. 7.  
 Gaisser, T. K., and Hillas, A. M. 1977, *Proc. 15th Internat. Conf. Cosmic Rays* (Plovdiv), **8**, 353.  
 Gaisser, T. K., Shibata, M., and Wrotniak, J. A. 1981, Rept. BA-81-21, Bartol Research Institute, University of Delaware.  
 Gaisser, T. K., and Stanev, T. 1989, private communication.  
 Gaisser, T. K., *et al.* 1990, in preparation.  
 Linsley, J. 1985, *Proc. 19th Internat. Conf. Cosmic Rays* (La Jolla), **7**, 167.  
 Linsley, J., and Watson, A. A. 1981, *Phys. Rev. Letters*, **46**, 459.

G. L. CASSIDAY, R. COOPER, S. C. CORBATÓ, B. R. DAWSON, J. W. ELBERT, B. E. FICK, K. D. GREEN, D. B. KIEDA, S. KO, E. C. LOH, M. H. SALAMON, J. D. SMITH, P. SOKOLSKY, P. SOMMERS, S. B. THOMAS, S. X. WANG, and B. WHEELER: Physics Department, University of Utah, Salt Lake City, UT 84112

D. F. LIEBING: WSRL, Defence Science and Technology Organization, Salisbury, S.A., Australia